Accepted for publishing in ASME Journal of Biomechanical Engineering in January 2007.

Optimal Combination of Minimum Degrees of Freedom to be Actuated in the Lower Limbs to Facilitate Arm-Free Paraplegic Standing

Joon-young Kim[1,3], James K. Mills[1], Albert H. Vette[2,3], and Milos R. Popovic[2,3]

[1] Department of Mechanical and Industrial Engineering, University of Toronto,
5 King's College Road, Toronto, Ontario, M5S 3G8, Canada

[2] Institute of Biomaterials and Biomedical Engineering, University of Toronto,
164 College Street, Toronto, Ontario, M5S 3G9, Canada

[3] Toronto Rehabilitation Institute, Lyndhurst Centre,
520 Sutherland Drive, Toronto, Ontario, M4G 3V9, Canada

Email: joonyoung.gim@gmail.com, mills@mie.utoronto.ca, a.vette@utoronto.ca, and milos.popovic@utoronto.ca

www.toronto-fes.ca

Corresponding Author:

Dr. Milos R. Popovic
Rehabilitation Engineering Laboratory
Institute of Biomaterials and Biomedical Engineering
University of Toronto
164 College Street, Room 407
Toronto, Ontario
Canada, M5S 3G9
Phone: +1-416-978-6676
Fax: +1-416-978-4317
Email: milos.popovic@utoronto.ca
www.toronto-fes.ca

Abstract

Background. Arm-free paraplegic standing via functional electrical stimulation (FES) has drawn much attention in the biomechanical field as it might allow an individual with paraplegia to stand and simultaneously use both arms to perform activities of daily living. However, current FES systems for standing require that the individual actively regulates balance using one or both arms, thus limiting the practical use of the proposed systems. The purpose of the present study was to show that actuating only six out of twelve degrees of freedom (DOF) in the lower limbs to allow individuals with paraplegia to stand freely is theoretically feasible with respect to multi-body stability and physiological torque limitations of the lower limb DOF. Specifically, the goal was to determine the optimal combination of the minimum DOF that can be realistically actuated in the lower limbs by means of FES, while ensuring stability and able-bodied kinematics during perturbed arm-free standing.

Method of Approach. The human body was represented by a three-dimensional dynamic model with twelve DOF in the lower limbs. *Nakamura's method*, a computationally efficient inverse dynamics method, was applied to estimate the joint torques of the system by means of experimental motion data from four healthy subjects. The torques were estimated by applying our previous finding that only six out of twelve DOF in the lower limbs need to be actuated to facilitate stable standing. Furthermore, it was shown that six cases of six active DOF (6-DOF) exist that facilitate stable standing. In order to characterize each of these cases in terms of the torque generation patterns and to identify a potential optimal 6-DOF combination, the joint torques during perturbations in eight different directions were estimated for all six cases of 6-DOF.

Results. The results suggest that the actuation of both ankle flexion/extension, both knee flexion/extension, one hip flexion/extension, and one hip abduction/adduction DOF will result in the minimum torque requirements to regulate balance during perturbed quiet standing.

Conclusions. To facilitate unsupported FES-assisted standing, it is sufficient to actuate only six DOF. An optimal combination of 6-DOF exists for which this system can generate able-bodied kinematics, while requiring lower limb joint torques that are producible using contemporary FES technology. These findings suggest that FES-assisted arm-free standing of paraplegics is theoretically feasible, even when limited by the fact that muscles actuating specific DOF are often denervated or difficult to access.

Keywords: balance, functional electrical stimulation, inverse dynamics, paraplegia, perturbed standing, quiet standing, torque estimation.

I. INTRODUCTION

A paraplegic is an individual whose spinal cord has been injured below the thoracic vertebra No.1, resulting in partial or complete loss of motor function in the lower limbs. The lost ability to stand can be regained by artificially stimulating the skeletal muscles in the lower limbs that cannot be controlled voluntarily [1]. However, for this to be possible, muscles targeted to be electrically stimulated must not be denervated, i.e., the axons that connect the muscles to their motor neurons in the spinal cord have to be intact[1]. Recently, arm-free standing of individuals with paraplegia using functional electrical stimulation (FES) has drawn much attention in the field of rehabilitation engineering as it might allow an individual with paraplegia to stand and at the same time use both arms to perform various activities of daily living (ADL) [2-4]. However, current FES systems for standing do not open up this possibility yet. Instead, they require that the individual actively regulates balance using one or both arms, thus limiting the use of the proposed FES systems during ADL [5,6].

Estimating the torques required at the joints of the lower limbs to allow stable standing is an important first step towards determining the feasibility of FES-assisted arm-free standing of individuals with paraplegia. Once the amount of torques needed during arm-free standing are known, the muscles capable of generating these torques can be identified. This would eventually assist in determining viable muscle stimulation strategies that an FES system for arm-free paraplegic standing should apply [7,8].

In general, there are two fundamental concepts in the field of biomechanics that are used to estimate the joint torques during human movement: forward and inverse dynamics. On the one hand, the forward dynamics method is used when it is of interest to determine

[1] Denervated muscles cannot be activated using conventional FES technology. They also degenerate over time and convert rapidly into fat and connective tissue.

how each muscle contraction affects the movement of the body [9,10]. One of the main difficulties associated with this method is to specify the control input that generates the joint torques responsible for the motion of the body. Additionally, in order to obtain this motion from the joint torques, the equations of motion of the dynamic model have to be integrated numerically [11,12]. On the other hand, the inverse dynamics method estimates the joint torques by solving a set of algebraic equations given the kinematics of the body [7,13]. As such, it is simpler to implement and computationally more efficient compared to the forward dynamics method.

The inverse dynamics method has been applied extensively to estimate joint torques during standing, especially when the analyses did not specifically require an understanding of the muscle coordination patterns. Although the precision of the inverse dynamics method has been improved by minimizing the error caused by imperfect kinematic measurement techniques [14,15], much work still remains to be done before the joint torques required for arm-free standing can be properly estimated. In particular, most of the dynamic models used in the literature ignore some important aspects of the actual quiet standing dynamics. First, almost all dynamic models neglect the three-dimensional[2] (3D), multi-body, closed-chain properties of quiet standing as described by Kim *et al.* [16,17]. Second, most joint torques estimated in the literature were determined for *all* degrees of freedom (DOF) of the model [11,13,15,18]. However, it may be difficult or even impossible to actuate all DOF in the lower limbs of individuals with paraplegia as some muscles may not be accessible or even denervated as described above. Hence, the minimum joint torques that are needed and that can actually be elicited by an FES system to allow individuals with paraplegia to stand, have not been properly estimated yet. That

[2] Note that *three-dimensional* implies a model articulation in three-dimensional space with three positional and three rotational degrees of freedom (x, y, and z; roll, pitch, and yaw).

is, it is not known how large the torques in the lower limbs of individuals with paraplegia must be to achieve FES-assisted arm-free standing, while avoiding the actuation of all DOF.

In our previous study [17], we developed a 3D dynamic model of the human body during double-support stance and found that only six out of twelve DOF need to be actuated in the lower limbs to facilitate stable arm-free standing despite moderate disturbances (i.e., disturbances that average healthy individuals should be able to compensate for without losing balance during standing). A total of six different cases of six active DOF (6-DOF) have been identified that would facilitate stable arm-free standing. Those six cases of 6-DOF were proposed in order to minimize the number of DOF that must be actuated by a potential FES system for paraplegic arm-free standing. However, it is certain that the six cases of 6-DOF will not generate identical torque patterns since each case consists of a different combination of DOF in the lower limbs.

Accordingly, in this manuscript, the joint torques were estimated using the inverse dynamics method for all six 6-DOF systems. The purpose was to show that actuating only six out of twelve DOF in the lower limbs to allow individuals with paraplegia to stand freely is theoretically feasible with respect to multi-body stability and physiological torque limitations of the lower limb DOF. Specifically, the goal was to determine the optimal 6-DOF combination that can be realistically actuated in the lower limbs by means of FES, while ensuring stability and able-bodied kinematics during perturbed arm-free standing.

Four able-bodied subjects participated in experiments that provided kinematic data describing the motion of healthy individuals during perturbed arm-free standing. The obtained time series were then used to calculate the joint torques for each case of 6-DOF by applying the inverse dynamics method. The recorded kinematic data were assumed to

be good examples of the desired behavior that a potential FES system for standing should be able to emulate.

The present study is organized as follows: First, the dynamic model and its inverse dynamics solutions obtained from our previous publication [17] are briefly introduced. Second, the formulation used for the joint torque calculation is validated. Third, the experimental method for obtaining the kinematics of the able-bodied subjects during perturbed arm-free standing is presented. Finally, the results of the joint torque estimation are presented and discussed.

II. METHODS

A. Three-Dimensional Dynamic Model

The 3D dynamic model of the human body during double-support stance, which has been developed in our previous study [17], is shown in Fig. 1. The HAT (Head-Arms-Trunk) was modeled as a rigid body with a constant mass and moment of inertia. Each leg consisted of six DOF, which has been shown to be a reasonable approximation of the double-support stance in humans [19]. The feet were not included in the model since it was assumed that the feet were fully in contact with the ground. Denavit-Hartenberg notation [20] was used for kinematic modeling, and Newton-Euler and Lagrange formulations were applied to the HAT and the legs, respectively, to obtain the dynamic model of the system. The equations of motion of the dynamic model shown in Fig. 1 are provided in the form of a set of first order ordinary differential equations (ODE):

$$\dot{\boldsymbol{x}} = \boldsymbol{f}(\boldsymbol{x}) \in \Re^{48\times 1} \tag{1}$$

Refer to Kim *et al.* [16,17] for more details on the dynamic model and Eq. (1).

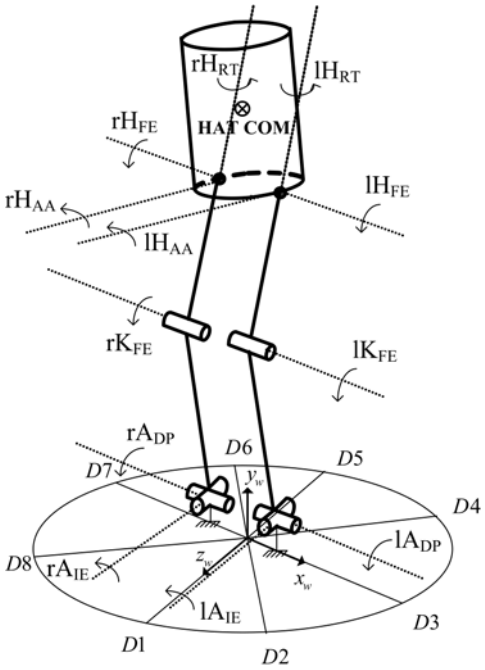

Fig. 1. 3D dynamic model of the human body during double-support stance [17]. The DOF of the joints are as follows: ankle inversion/eversion (lA_{IE}, rA_{IE}); ankle dorsiflexion/plantarflexion (lA_{DP}, rA_{DP}); knee flexion/extension (lK_{FE}, rK_{FE}); hip abduction/adduction (lH_{AA}, rH_{AA}); hip flexion/extension (lH_{FE}, rH_{FE}); and hip rotation (lH_{RT}, rH_{RT}). The system was perturbed in eight different directions, D1 to D8.

B. Inverse Dynamics Solutions

By applying Nakamura's method [21], the inverse dynamics solution for the dynamic model shown in Fig. 1 was obtained in [17] as

$$\boldsymbol{\tau}_a = W^T \left(\boldsymbol{M}_t \ddot{\boldsymbol{q}} + \boldsymbol{C}_t \dot{\boldsymbol{q}} + \boldsymbol{N}_t \right) \in \Re^{N_a \times 1}, \tag{2}$$

where $\boldsymbol{W} := \begin{bmatrix} \boldsymbol{I} \\ -\boldsymbol{J}_p^{-1} \boldsymbol{J}_a \end{bmatrix} \in \Re^{12 \times N_a}$; $\boldsymbol{I} \in \Re^{N_a \times N_a}$: identity matrix; $\boldsymbol{q} := \begin{bmatrix} \boldsymbol{q}_a & \boldsymbol{q}_p \end{bmatrix}^T \in \Re^{12 \times 1}$; $\boldsymbol{q}_a \in \Re^{N_a \times 1}$: active DOF; $\boldsymbol{q}_p \in \Re^{N_p \times 1}$: passive DOF, i.e., zero torque at the passive DOF; N_a: number of active DOF; N_p: number of passive DOF; $\boldsymbol{\tau}_a \in \Re^{N_a \times 1}$: torque at active DOF; $\boldsymbol{J}_a \in \Re^{6 \times N_a}$: Jacobian matrix with respect to the active DOF; $\boldsymbol{J}_p \in \Re^{6 \times N_p}$: Jacobian matrix with respect to the passive DOF; $\boldsymbol{M}_t(\boldsymbol{q}) \in \Re^{12 \times 12}$: inertia matrix; $\boldsymbol{C}_t(\boldsymbol{q}, \dot{\boldsymbol{q}}) \in \Re^{12 \times 12}$:

Coriolis-centrifugal force matrix; and $\boldsymbol{N}_t(\boldsymbol{q}) \in \Re^{12\times 1}$: gravity vector. The details of Eq. (2) can be found in [16,17].

According to (2), as long as $N_a \geq 6$ and $rank(\boldsymbol{J}_p) = 6$, the inverse dynamics solution of the model in Fig. 1 exists, i.e., unique $\boldsymbol{\tau}_a$ can be calculated for the given system kinematics. The analysis conducted using kinematic data obtained in experiments with able-bodied subjects suggests that six combinations of 6-DOF exist for which the system $\boldsymbol{J}_p$ has a rank equal to six for any given able-bodied, arm-free standing kinematics. Hence, six DOF is the minimum number of DOF that need to be actively controlled during perturbations to facilitate stable arm-free standing. The combinations of the six actively controlled DOF as shown in Fig. 2 were obtained based on the assumption that lA_{IE}, rA_{IE}, lH_{RT}, and rH_{RT} are always passive DOF. This assumption is reasonable as these DOF are difficult to actuate with contemporary transcutaneous FES technology [5,6,22]. Due to the symmetry of the two legs, each case shown in Fig. 2 also represents the 6-DOF combination of its mirror image. Note that the presented findings have been initially reported in [17].

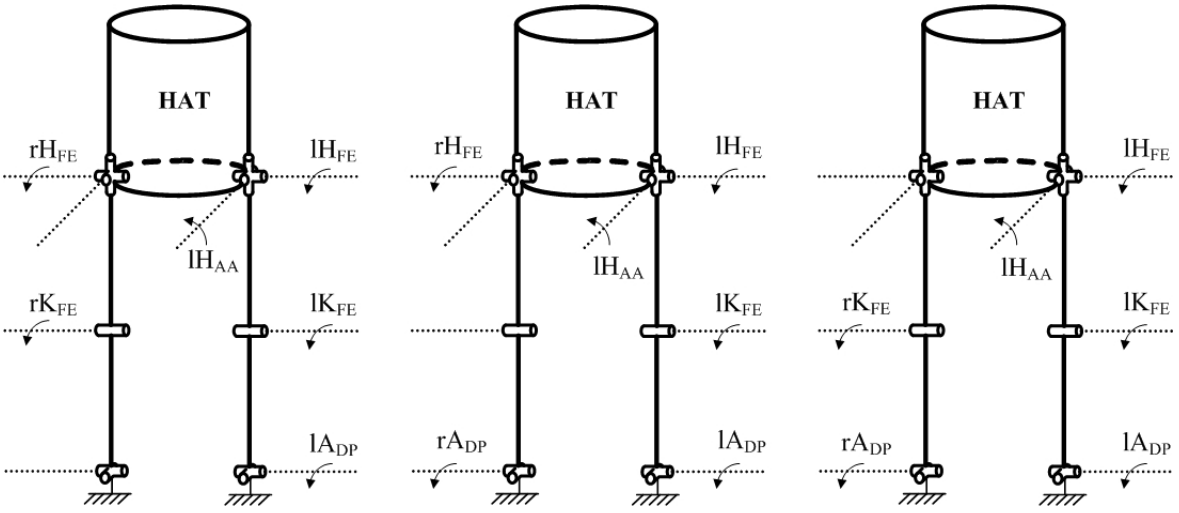

Case I **Case III** **Case V**

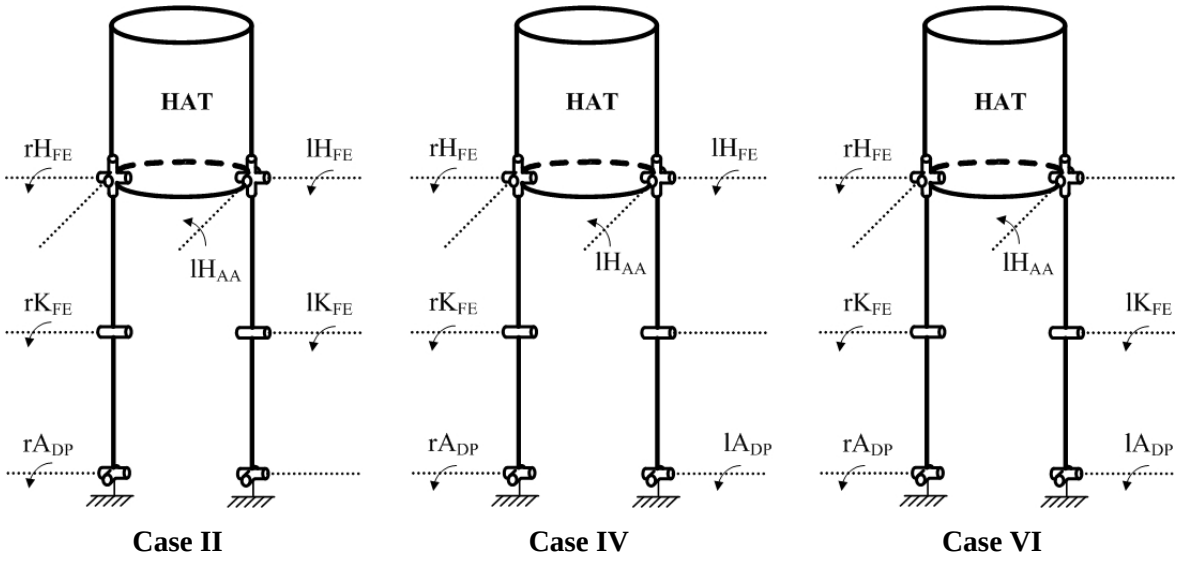

Fig. 2. Six cases of 6-DOF such that the passive Jacobian matrices are not singular [17]. Note that, due to the symmetry of the two legs, each case also represents the 6-DOF combination of its mirror image. For example, Case I also stands for the combination of lK_{FE}, lH_{FE}, rA_{DP}, rK_{FE}, rH_{AA}, rH_{FE} as active DOF.

C. Internal Validity of the Model

Due to its complexity, the formulation for estimating the joint torques (Eq. (2)) was validated using the internal validity test, i.e., by comparing the forward and inverse dynamics of the model [7]. However, the internal validity test is known to be of limited value if the same equations are used in the forward and inverse dynamics, since the two methods will still match theoretically in spite of potential errors in the formulation [23]. Therefore, different methods were used for testing the internal validity. That is, the Newton-Euler and Lagrange methods were used for the forward dynamics (Eq. (1)), and Nakamura's method was used for the inverse dynamics (Eq. (2)).

Even if the formulation is provided without an error, it is very likely that the forward and inverse dynamics during simulation will not match [9,11]. This phenomenon has been referred to as *inverse dynamics simulation failure* [23]. Although it is not clearly understood why such matching of ideal forward and inverse dynamics models may fail,

two potential causes have been suggested in the literature: (a) the insufficient dimensionality of the control signal and/or (b) the unstable equation of motion. Both these phenomena are linked to the forward dynamics calculations [23]. To eliminate one potential source for mismatch in the inverse and forward dynamic calculations, a small, fixed simulation step-size of 0.001 s was applied to reduce the error introduced by discrete numerical integration. Additionally, the *torque control algorithm* [24] was applied to stabilize the unstable Eq. (1). That is, the kinematics, i.e., the input of the inverse dynamics, were set as the reference trajectory that the dynamic system in (1) should generate in the forward dynamics. Note that this scheme guarantees the asymptotic stability of the forward dynamics with respect to the reference trajectory [24]. As a final step of the internal validation, the input and output of the forward and inverse dynamics were compared. In order to perform the numerical simulations, Adams' method for solving ODEs was used. However, since Adams' method is a multi-step method, a single-step method was needed to start up the simulation. This was accomplished using a 4^{th} order Runge-Kutta method. Please refer to Kim [16] for details.

In Fig. 3, the results of the internal validity test are shown for Case VI. The inputs of the forward dynamics demonstrated the same patterns as the outputs of the inverse dynamics and vice versa. The total average error between the test kinematics and the output of the forward dynamics was $5.6 \cdot 10^{-5}$ degrees (12 DOF for six cases), whereas the total average error between the control input of the forward dynamics and the output of the inverse dynamics was 0.89 Nm (6 active DOF for six cases). As such, the formulations of Eq. (1) and Eq. (2) were validated.

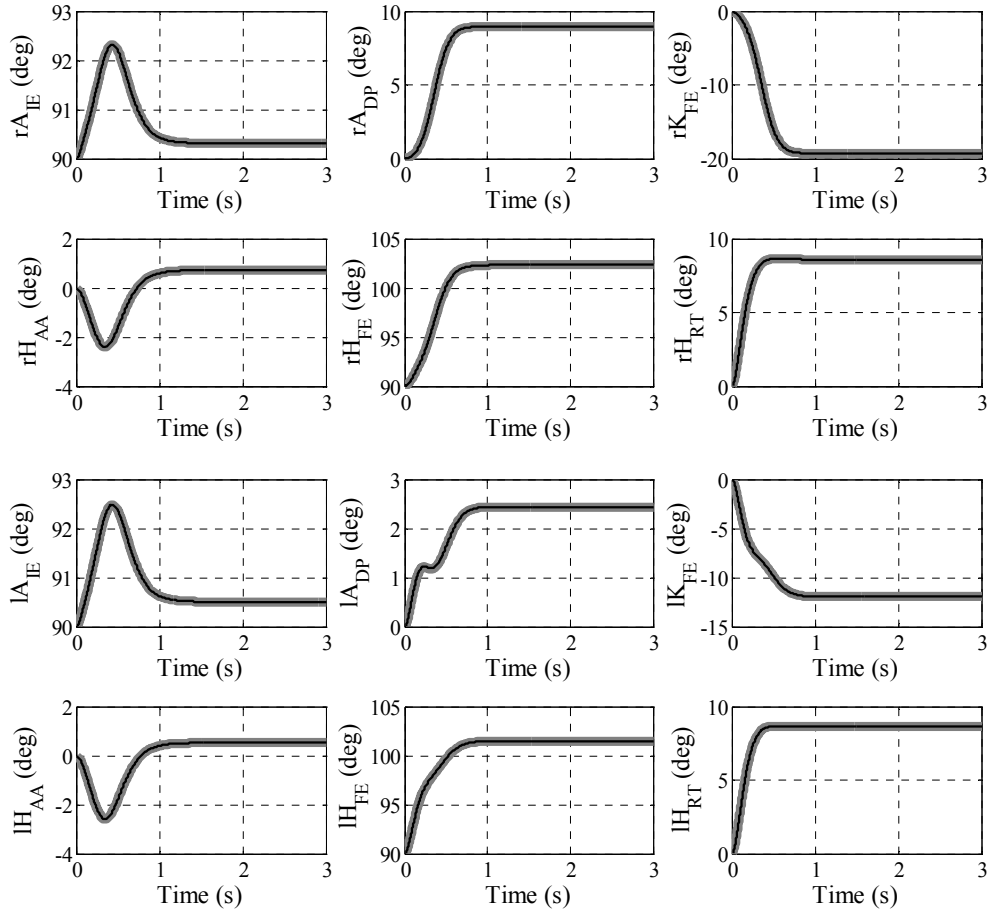

(a) Test kinematics and output of the forward dynamics.

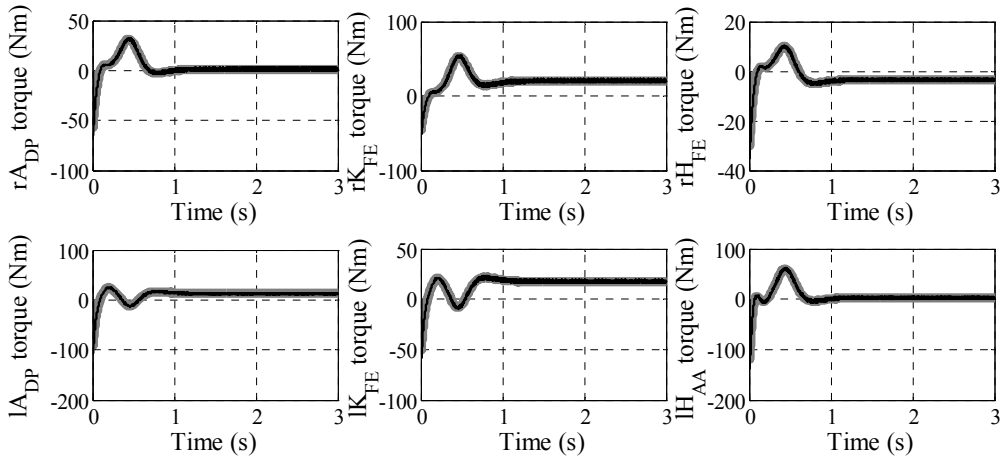

(b) Output of the inverse dynamics and control input of the forward dynamics.

Fig. 3. Internal validity test for Case VI in Fig. 2. The thick gray lines indicate the inputs and outputs of the inverse dynamics and the thin black lines indicate those of the forward dynamics. Note that the validation test was performed for all six cases of 6-DOF.

D. Acquisition of Able-Bodied Kinematics during Perturbed Standing

In order to estimate the joint torques by solving Eq. (2), it was necessary to obtain the body kinematics during perturbed arm-free standing. Since the purpose of the inverse dynamics problem was to estimate the joint torques in the lower limbs of an individual with paraplegia such that they generate the same standing motion as in healthy individuals, four healthy subjects were invited to participate in the experiments. Table 1 describes the height, weight, age, and sex of each subject. The experiments were approved by the ethics boards of the University of Toronto and the Toronto Rehabilitation Institute, Canada. Informed consent was obtained from the subjects prior to the experiments.

Table 1. Height, Weight, Age, and Sex of the Four Able-Bodied Subjects.

Subject	Height (m)	Weight (kg)	Age (yr)	Sex
S1	1.71	66.7	32	F
S2	1.65	63.6	31	F
S3	1.93	116.2	32	M
S4	1.66	63.3	31	F

During the experiment, each subject was asked to stand with bare feet in the most comfortable standing posture with his/her eyes closed and the arms folded on the chest. In order to obtain an accurate 3D representation of the kinematics during standing, the subject was perturbed using an impulse-like force acting in eight directions (D1 to D8 in Fig. 1). The perturbation system consisted of a drop weight of 4.54 kg, a pulley and a rope that was attached to the subject at the level of his/her center of mass (COM). The height of the pulley was adjusted depending on the height of the subject so that the perturbation direction was always parallel to the ground. For each perturbation direction, the rope connected to the waist of the subject was cocked (zero slack), suddenly pulled by releasing the drop weight, and then slackened in order to generate impulse-like perturbations. Note

that only those trials were accepted for which the perturbation force acting on the subject's body lasted between 0.7 and 1 s, resulting in a force sum between 31.2 and 44.5 Ns. This methodology was ensured by tracking the motion of reflective markers on the rope and drop weight using a motion analysis system (Optotrak 3020, Northern Digital Inc., Canada). The subject was perturbed three times for each direction, resulting in a total of 24 trials per subject. During all trials, it was ensured that both feet of the subject remained in contact with the ground at all times.

The aforementioned motion analysis system was used to record the joint angles of the body segments with a sampling frequency of 100 Hz. Custom-designed rigid bodies were used to place the reflective markers on the body. Five rigid bodies were attached to the shanks, thighs, and torso of the subject. The joint angles were filtered using a fourth-order, zero-lag Butterworth filter with a cut-off frequency of 2 Hz, which was determined by a power spectrum analysis of the measured joint angles. The angular velocities and accelerations were then estimated by the *finite differentiation technique* [7]. Using this method in combination with a low-pass digital filter is known to be very efficient in estimating the derivatives of the measured joint angles [25,26]. The lengths of the body segments of each subject were measured before the experiments, whereas the mass, the moment of inertia, and the location of the COM of each body segment were estimated based on the subject's anthropometric data [7]. The moments of inertia of the body segments that could not be obtained from the anthropometric data, e.g., trunk rotation about the vertical axis, were estimated by approximating the body segment using a cylinder. By means of the kinematic data and the anthropometric parameters of the subjects, the joint torques of the minimum number of DOF were calculated for all eight

perturbation directions and all six cases shown in Fig. 2 by solving Eq. (2), i.e., the inverse dynamics method.

E. Analysis of Joint Torques

The analysis of the joint torques identified by means of the kinematic data and inverse dynamics method was focused on investigating how each case of 6-DOF shown in Fig. 2 was different from the other five cases. Specifically, we identified differences in (a) the direction of and (b) the intensity of the stabilizing joint torques, as these were the primary factors that characterized each case of 6-DOF. A norm based measure for each active DOF's torque profile was determined by numerically integrating the norm of the torque as a function of time over an interval of five seconds, i.e., $\int_0^5 |\boldsymbol{\tau}_a| dt$ (Nm·s), where $\boldsymbol{\tau}_a$ is the active DOF's mean torque as a function of time obtained from the three perturbation experiments per subject. An integration interval of 5 s was used since all four subjects regained balance and assumed a quiet standing posture within a time period shorter than 5 s. The value of $\int_0^5 |\boldsymbol{\tau}_a| dt$ is referred to in the paper as *torque sum*. For each perturbation direction, the torque sums were first determined for each subject (three trials each), but then averaged over all four subjects, i.e., over twelve trials (referred to as *average torque sum*). The average torque sums are given as mean ± standard deviation.

III. RESULTS

A. Anterior-Posterior (A/P) Perturbations

In the case of perturbations in the A/P direction (D1 and D5), it was discovered that Cases I and II (Fig. 2) generated equivalent torque profiles in response to each perturbation. A similar behavior was observed for Cases III and IV as well as for Cases V and VI. This can be explained by the fact that these pairs have the same combinations of those five active DOF that have their axes of rotation orthogonal to the sagittal plane (Fig. 2). Furthermore, the torque at lH_{AA} was relatively small compared to the torques at the other DOF for the D1 and D5 perturbations. Thus, the joint torques were analyzed for three groups: Group A (Cases I and II), Group B (Cases III and IV), and Group C (Cases V and VI). The only difference between the two cases in each group was the number of the DOF per leg that have their axes of rotation orthogonal to the sagittal plane, i.e., the DOF corresponding to the movement in the A/P direction. Therefore, the legs were labeled as 3DOF-leg and 2DOF-leg such that the 3DOF-leg had three DOF and the 2DOF-leg had two DOF in the A/P direction. For example, in Case I the left leg is the 3DOF-leg and the right leg the 2DOF-leg (Fig. 2).

1) Perturbation in D1 Direction

Group A

As shown in Fig. 2, the A/P DOF in case of Group A consisted of one ankle dorsiflexion/plantarflexion DOF (A_{DP}), two knee flexion/extension DOF (K_{FE}), and two hip flexion/extension DOF (H_{FE}). In this group, the torques at A_{DP}, K_{FE}, and H_{FE} in the 3DOF-leg were first increased (+) at the onset of the D1 perturbation, then decreased (–), and then increased (+) again to generate the corresponding joint angles (Fig. 4.a and 4.b). However, the torques at K_{FE} and H_{FE} of the 2DOF-leg were suddenly decreased (–), then

increased (+), and then decreased (–) again. Thus, the joint torques at the two A/P DOF of the 2DOF-leg were generated in the opposite direction to the ones at the three A/P DOF of the 3DOF-leg. Although the results of only one subject (S1) are shown in Fig. 4, the above phenomenon was observed for all subjects.

The average torque sums for Group A are shown in Fig. 5.a (upper values). It was found that the overall average torque sum of the 3DOF-leg was much higher (5.2 ~ 6.7 times) than the one of the 2DOF-leg. The above results suggest that the 3DOF-leg in Group A must account for most of the torques that are necessary to stabilize the body after the D1 perturbation. The torques at the two DOF of the 2DOF-leg, i.e., K_{FE} and H_{FE}, must be generated in the opposite direction in order to compensate for the internal kinematic constraints of the system.

Group B

In case of Group B, the A/P DOF consisted of two A_{DP}, one K_{FE}, and two H_{FE} (Fig. 2). At the onset of the D1 perturbation, the torques at all DOF, except for H_{FE} of the 2DOF-leg, were suddenly increased (+), then decreased (–), and then increased (+) again (Fig. 4.a and 4.c). As for the torque at H_{FE} of the 2DOF-leg, it was first decreased (–), then increased (+), and then decreased (–) again (Fig. 4.c).

The overall average torque sum for Group B was similar to the one for Group A in that most of it was generated in the 3DOF-leg, i.e., it was 5.7 ~ 7.6 times higher than the overall average torque sum of the 2DOF-leg (Fig. 5.b). In comparison with Group A, only the torque at H_{FE} in the 2DOF-leg acted in the opposite direction in Group B. Note that there were two DOF in Group A that acted in the opposite direction. In addition, it was found that Group B generated smaller torques as the overall average torque sum of all the A/P DOF in Group B was smaller by 7 % ~ 12 % than in the case of Group A (Fig. 5.b).

Group C

In Group C, the A/P DOF consisted of two A_{DP}, two K_{FE}, and one H_{FE}. Note that in each of the other two groups two H_{FE} were actuated, whereas in this case only one H_{FE} was actuated. Figure 4.d shows that all five DOF in this group had the same torque direction, i.e., the torque increased (+) at the onset of the perturbation, then decreased (–), and then increased (+) again. As such, there were no torques at the 2DOF-leg DOF in Group C that counteracted the torques of the 3DOF-leg DOF. Note that there was at least one 2DOF-leg DOF in groups A and B at which the torque was generated in the opposite direction.

The average torque sum analysis demonstrated that the torques were distributed more evenly between the legs than in the other groups, i.e., the overall average torque sum of all A/P DOF in the 3DOF-leg was only 2.3 ~ 3.4 times higher than that of the 2DOF-leg (Fig. 5.c). The overall average torque sum of all A/P DOF was reduced by up to 22 % ~ 27 % compared with Group A. Therefore, Group C produced the lowest overall torque sum for the D1 perturbation, whereas Group A generated the largest overall torque sum.

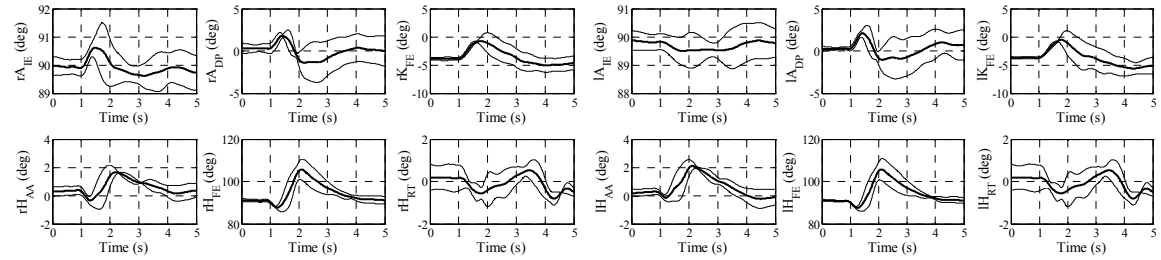

(a) Joint angles

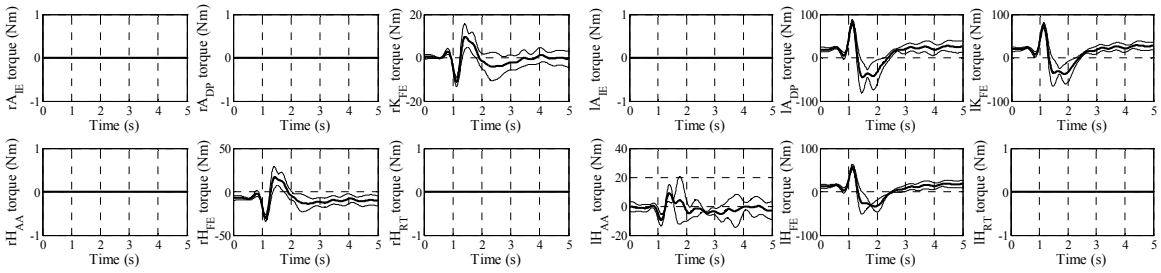

(b) Joint torques for Group A (Case I)

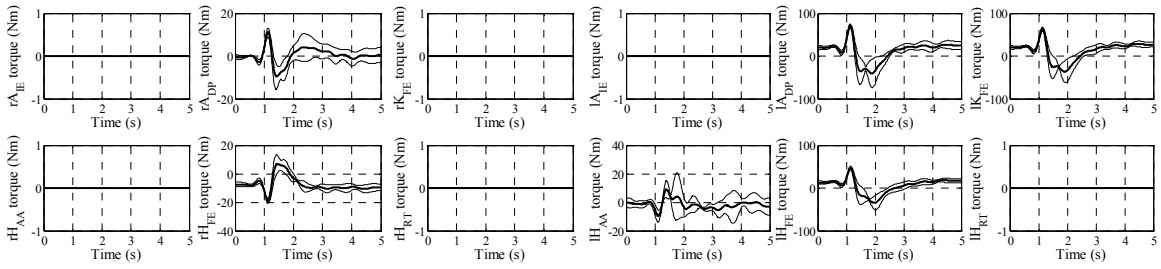

(c) Joint torques for Group B (Case III)

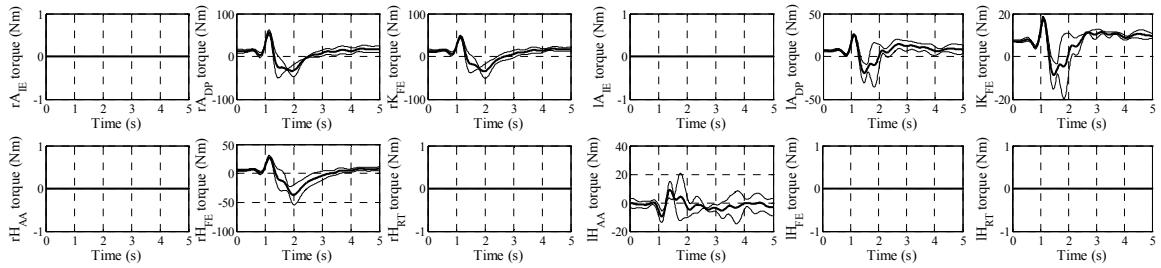

(d) Joint torques for Group C (Case VI)

Fig. 4. Joint angles and joint torques of subject S1 at the six actuated DOF due to the perturbation given in direction D1. The mean values with one standard deviation from three trials are shown as a function of time.

2) Perturbation in D5 Direction

Only two subjects (subjects S1 and S3) were able to maintain balance during the perturbation in the D5 direction. Subjects S2 and S4 failed to keep their feet on the ground in all three perturbation trials. Figure 5 shows that the average torque sum due to the D5 perturbation was much higher than the one due to the D1 perturbation. This explains why the two subjects S2 and S4 were unable to maintain balance in case of the D5 perturbation. Note that subjects S2 and S4 were not as tall as subjects S1 and S3 (Table 1).

For the D5 perturbation, the characteristics of the torque direction for the three groups were consistent with the results of the D1 perturbation. That is, Group A and B had the same DOF as for the D1 perturbation at which the torques were generated in the opposite direction, whereas in Group C all A/P DOF acted in the same direction. Group B produced an overall torque sum that was 12 % ~ 18 % larger than for Group A. The overall torque sum of all the A/P DOF in Group C was smaller than in Group A by 15 % ~

17 %. Therefore, Group C required the lowest overall torque sum to maintain balance during the D5 perturbation, whereas Group B required the largest overall torque sum (Fig. 5, lower values).

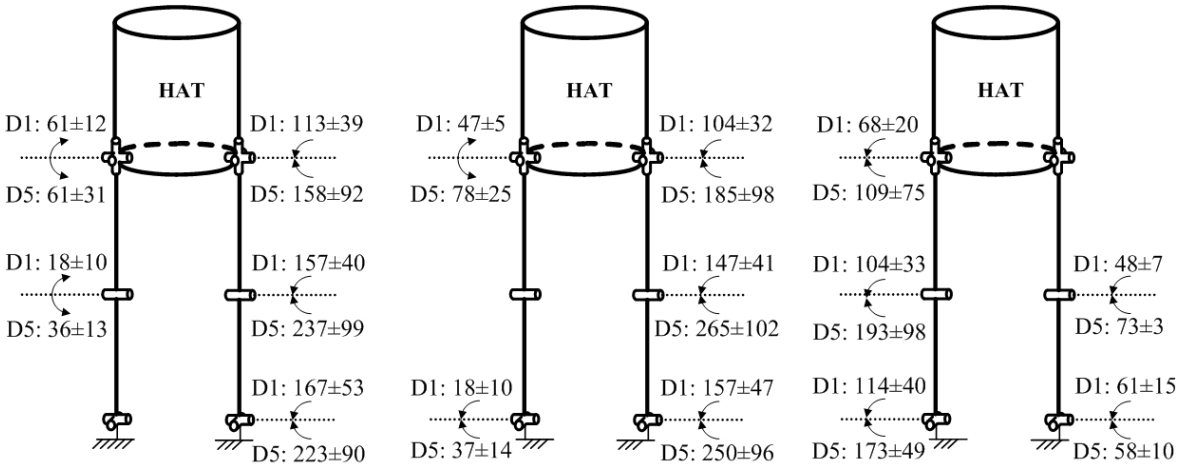

(a) Group A (Case I) (b) Group B (Case III) (c) Group C (Case VI)

Fig. 5. The average torque sums for each A/P DOF and each group that were generated due to the A/P perturbations. The average torque sum with standard deviation (*Nm·s*) from four subjects (twelve trials) is shown, i.e., the torque generated due to the perturbation in the D1 (upper arrow and torque value) and D5 (lower arrow and torque value) directions. Notice the difference of the arrow directions.

B. Medio-Lateral (M/L) Perturbations

In the case of the M/L perturbations (D3 and D7 directions), all subjects moved predominantly in the M/L direction, whereas the movement in the A/P direction was relatively small (Fig. 6.a). Since each group had only one M/L DOF, i.e., the hip abduction/adduction DOF (H_{AA}) as depicted in Fig. 2, it could be expected that the torque pattern at this DOF was the same for all three groups during the M/L perturbations. In fact, the torque at H_{AA} exhibited similar characteristics for all subjects regardless of the location of H_{AA} (left or right leg). That is, at the onset of the perturbation in the D3 direction, the torque was suddenly increased (+), then decreased (–), and then increased (+) again to obtain the specified joint angles (Fig. 6.a and 6.b). Moreover, the six cases of 6-

DOF shown in Fig. 2 did not demonstrate any differences with respect to the average torque sum and, and as such, the average torque sum did not depend on the location of H_{AA}.

However, the average torque sum of the A/P DOF depended on the combination of the active DOF. That is, Group C generated as for the A/P perturbations the least torque sum at the A/P DOF compared to the other two groups. As a result, Group C generated also the lowest *overall* torque sum among the three groups since (a) it generated the least overall torque sum at the A/P DOF and (b) the torque pattern at H_{AA} (corresponding to the only M/L DOF) was equal for all three groups in the case of the M/L perturbations. This suggests that the results of the torque analysis for the perturbations in the A/P directions also hold for the perturbations in the M/L directions.

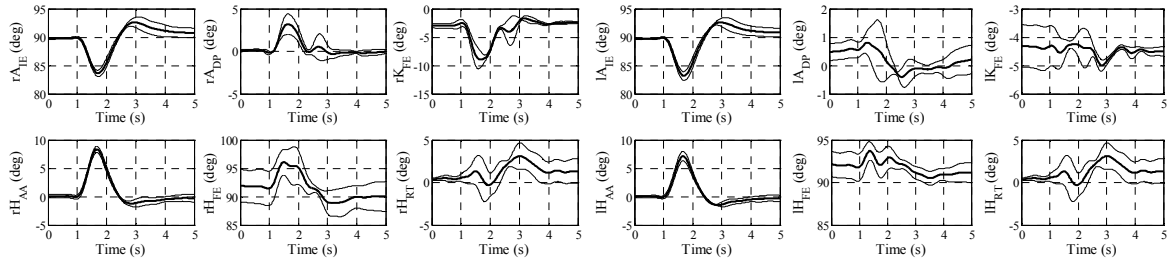

(a) Joint angles

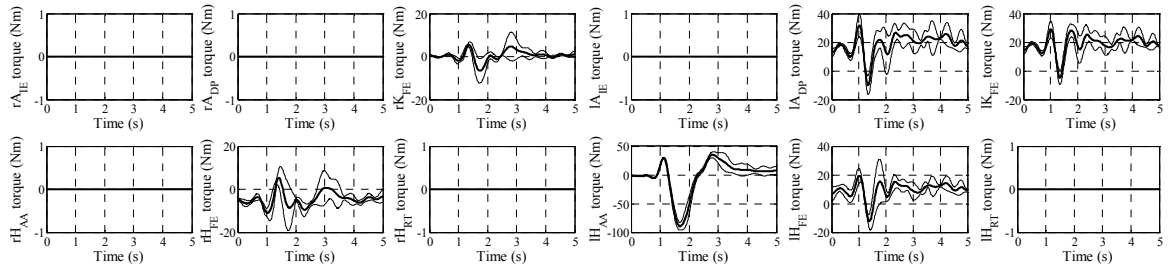

(b) Joint torques for Group A (Case I)

Fig. 6. Joint angles and joint torques of subject S1 at the six actuated DOF due to the perturbation given in direction D3. The mean values with one standard deviation from three trials are shown as a function of time. Since the torque characteristics at H_{AA} where identical for all three cases, only Case I is shown.

C. Perturbations in Diagonal Directions

For the perturbations in the diagonal directions (D2, D4, D6, and D8 in Fig. 1), all subjects moved along a trajectory that combined both the A/P and M/L directions (Fig. 7.a). That is, the movements observed in the subjects due to the perturbations in the forward (D2 and D8) and backward (D4 and D6) diagonal directions represented the combinations of those in the D1 and M/L directions and those in the D5 and M/L directions, respectively. Thus, it was expected that the torque patterns in the case of the diagonal perturbations would be composed of the torque patterns observed during the disturbances along the A/P and M/L directions.

In fact, the characteristics of the torque directions of the A/P DOF in the case of the D2 and D8 perturbations were the same as those observed in the case of the D1 perturbations. Similarly, the characteristics of the torque directions of the M/L DOF in the case of the D2 and D8 perturbations were the same as those observed in the case of the M/L perturbations (Fig. 7.b). The same result was obtained for the perturbations in the backward diagonal directions (D4 and D6). These characteristics were consistent for all trials of all four subjects.

The analysis of the average torque sums revealed that Group C had the lowest overall torque sum at the A/P DOF for both the forward (D2 and D8) and backward (D4 and D6) diagonal perturbations. Group A and Group B produced the largest overall torque sums at the A/P DOF in the forward and the backward diagonal directions, respectively. Moreover, the average torque sums at the M/L DOF were the same for all three groups and all diagonal perturbations.

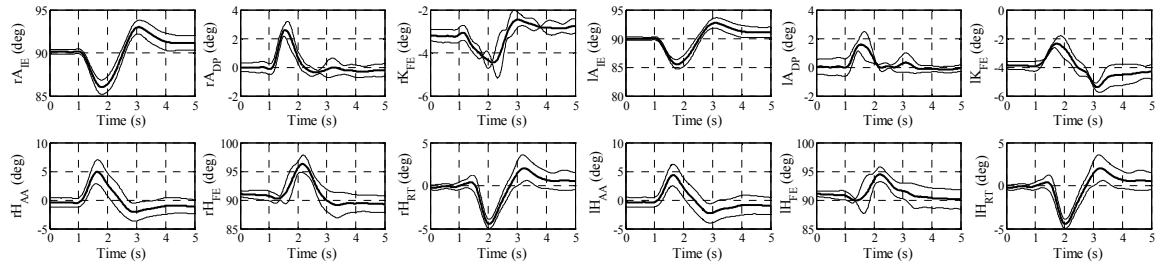

(a) Joint angles

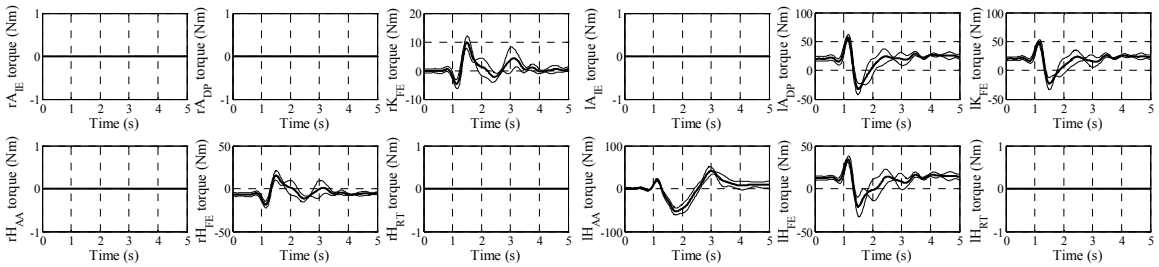

(b) Joint torques for Group A (Case I)

Fig. 7. Joint angles and joint torques of subject S1 at the six actuated DOF due to the perturbation given in direction D2. The mean values with one standard deviation from three trials are shown as a function of time. Since the torque patterns were composed of the patterns during the A/P and M/L perturbations (Fig. 4 and 6), only Case I is shown.

D. Summary

In Fig. 8, the overall torque sums calculated for all eight perturbation directions (Fig. 1) and all six cases of six active DOF (Fig. 2) are presented. As described, Group C (Cases V and VI) generated the lowest overall torque sum at all six active DOF. Moreover, Groups A (Cases I and II) and B (Cases III and IV) generated the largest overall torque sum at all active DOF for the forward perturbations (D1, D2, and D8) and the backward perturbations (D4, D5, and D6), respectively.

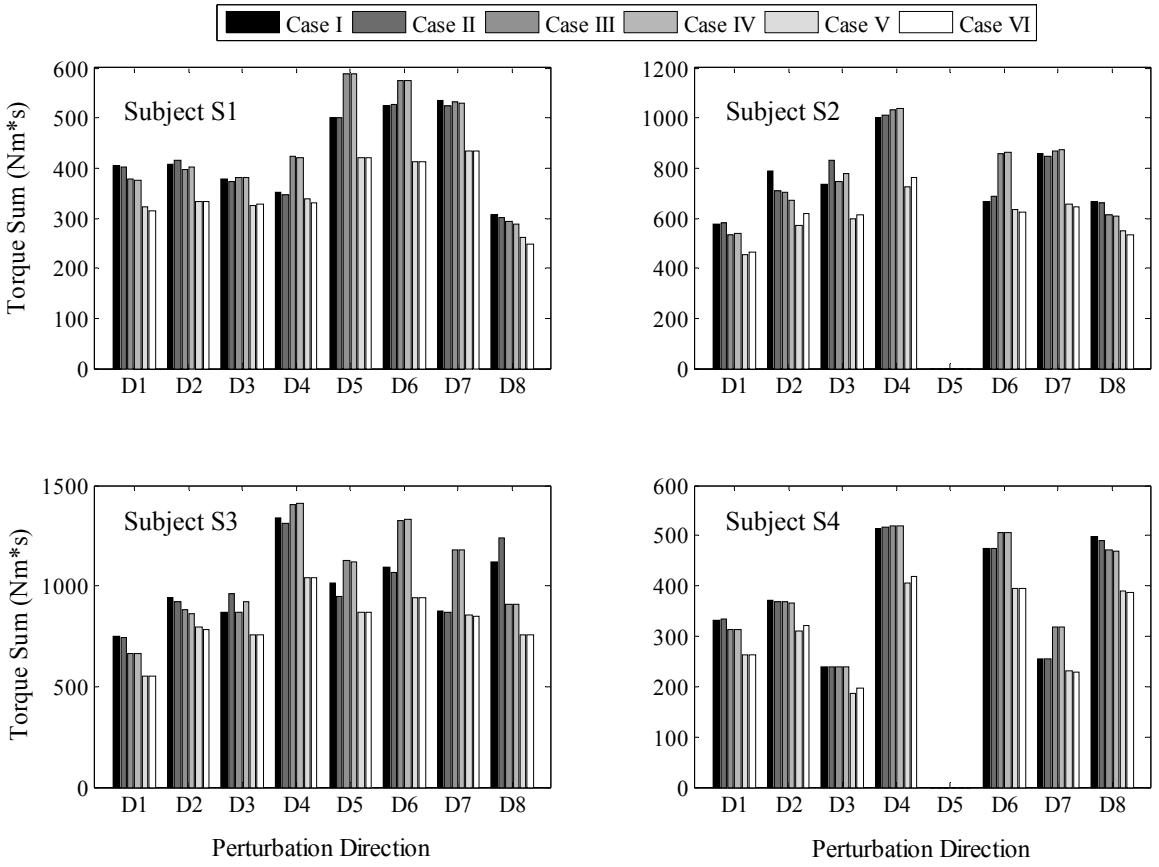

Fig. 8. Torque sums of the joint torques at all active DOF, shown for each of the six 6-DOF systems (Cases I to VI) and all directions of perturbation (D1 to D8). Note that subjects S2 and S4 show overall torque sums for seven perturbation directions only as these subjects lost balance during the D5 perturbations. Recall that Cases I and II represent Group A, Cases III and IV represent Group B, and Cases V and VI represent Group C.

IV. DISCUSSION

The joint torque estimation is a crucial step in developing and implementing a practical FES system for paraplegic standing as it is necessary for determining feasible muscle stimulation strategies. However, the joint torques that are needed in the particular application of FES-assisted paraplegic arm-free standing have not been properly estimated yet. Most studies in the literature attempting to do so used planar instead of three-dimensional dynamic models and did not consider some important dynamic aspects during quiet standing such as 3D multi-body closed-chain dynamics. Others estimated the torques for *all* DOF occurring in the dynamic model. The problem associated with this approach is that some muscles in the lower limbs are very difficult to access, whereas others might be denervated in individuals with paraplegia. As a result, also the corresponding DOF such as the hip rotation or ankle inversion/eversion DOF might be very problematic to control. Furthermore, when the torques are estimated for *all* DOF, one has to assume a particular optimization method in order to resolve the redundancy problem associated with the system of bipedal stance. However, it is not known which optimization technique should be applied since the activation patterns observed in experiments do not resemble the output of proposed optimization techniques [27]. Due to these limitations, the objective of the present study was to use a realistic, 3D nonlinear dynamic model of quiet standing to determine those combinations of the minimum number of active DOF that (a) facilitate stable arm-free standing and generate able-bodied kinematics during moderate disturbances; (b) can be activated and controlled in individuals with paraplegia using contemporary FES technology; and (c) minimize the muscle forces and energy spent to prevent fatigue and allow for prolonged periods of stable standing.

The most significant result obtained from the joint torque estimation is that there exist optimal cases among the 6-DOF combinations (Fig. 2) such that the overall torque sum was lowest and most evenly distributed among the two legs for all eight directions of perturbation. These optimal combinations, Cases V and VI in Fig. 2, consisted of one H_{AA}, one H_{FE}, two K_{FE}, and two A_{DP}. Note that these two cases actually imply four different optimal combinations as each case in Fig. 2 has a counterpart due to the symmetry of the two legs. Cases I to IV on the other hand had two H_{FE}, thus missing one A/P DOF to be actuated in either the ankle or knee joint. The joint torque patterns of Cases V and VI were fundamentally different from the other cases in that the torque of all the active A/P DOF acted together in the same direction, whereas in the other cases at least one DOF existed that was actuated in the opposite direction due to the closed-chain dynamics. Although the two legs generated almost the same motion (e.g. Fig. 4.a), counteracting torques were necessary in Cases I through IV to account for the existence of passive DOF in the closed-chain dynamic system. More specifically, when there was one passive A/P DOF at the ankle or knee joint, some DOF had to be actuated in the opposite direction to that of the remaining active DOF in order to allow the desired movement at the passive ankle or knee DOF. Since this was not necessary in Cases V and VI, it seems plausible that these two cases require less amount of torque compared to the other four cases.

Due to space limitations and the primarily theoretical nature of our study, we decided not to include an analysis of inter- and intra-subject variability in our methods. Nevertheless, it has to be said that the torque characteristics, i.e., the torque directions and torque sum distributions, were identical across trials and subjects for *all* directions of perturbation and *all* cases of 6-DOF. Since this implies agreement in more than hundred conditions, it can be assumed that the results are not affected by inter- and intra-subject

variability. Please refer to Kim [16] for the complete joint angle and joint torque profiles for all subjects, perturbation directions, and cases of 6-DOF.

Due to the fact that only six out of twelve DOF would have to be actuated in a practical FES system, it must also be expected that larger torque peaks are necessary for asymptotic stability in comparison with the theoretical case where all twelve DOF are being actuated. As such, it has to be ensured that the required torque levels in Cases V and VI can actually be generated by means of FES. In order to do so, we determined the largest stabilizing torque peak at the A/P DOF during the D1 perturbation (Fig. 4.d) as well as at the M/L DOF during the D3 perturbation (Fig. 6.b) and discussed whether these torque levels can be generated by means of contemporary FES technology. Note that these combinations represent the cases where the DOF act in the same direction as the perturbation, and therefore the largest torque peaks can be expected.

During the D1 perturbation, A_{DP} at the 3DOF-leg generated the largest stabilizing torque peak (negative peak of rA_{DP} in Fig. 4.d). It had a value of –33 Nm and represented the maximum torque that the plantar flexors would have to generate for an equivalent subject to compensate for the perturbation force. In previous experiments carried out in our laboratory, we tested whether this torque level can be generated using FES. Our results show that the calculated torque maximum of 33 Nm (Fig. 4.d) could be elicited without difficulties in an untrained SCI subject (von Hippel-Lindau disease) using contemporary surface FES technology [28]. In our experiments, we applied asymmetric biphasic pulses with a pulse width of 300 μs, a frequency of 35 Hz, and amplitudes ranging from 20 to 48 mA. The stimulation was applied using a Compex Motion surface FES system [29] and 10 cm × 5 cm self-adhesive transcutaneous electrodes. During the experiments, the ankle torques were measured using a Biodex torque dynamometer

(Biodex Medical Systems, Shirley, NY). For the above stimulation parameters, we were able to generate up to 52 Nm of plantar flexion torque in the SCI subject. Since it is common in practical FES applications to use higher stimulation amplitudes and frequencies as well as smaller electrodes (5 cm × 5 cm) than the ones used in these experiments, even larger plantar flexion torques may be achieved if required.

During the D3 perturbation, the compensating torque at H_{AA} had a maximum value of –90 Nm (lH_{AA} in Fig. 6.b). Although this peak is specifically required for the 6-DOF system in Case I, it is also applicable for Cases V and VI since H_{AA} was the only M/L DOF in all 6-DOF systems, generating similar responses to the D3 perturbation for all six cases (see *B) Medio-Lateral (M/L) Perturbations*). Marsolais and Kobetic showed in 1988 that a percutaneous FES system stimulating the hip abductors of a subject with a neurologically complete T9 injury could generate more than sufficient torque to overcome gravity [30]. Taking the mass and moment arm of the subject's leg into account, we are confident that the aforementioned torque peak at H_{AA} can be generated with more advanced, contemporary FES technology.

Due to these findings, it is, in fact, feasible to generate the required torques at the six active DOF that are needed to maintain standing stability after moderate disturbances. Moreover, the required torque levels can be reduced by implementing a conservative torque control scheme that reduces the maximum torque output while retaining good perturbation rejection properties [17]. Such a control scheme would take the unique case into account that not all, but only six DOF are actuated. As a result, also the generated kinematics would be unique and might not exactly represent the ones of healthy individuals where usually twelve DOF are actuated. It has also to be noted that the torques

calculated in the present study represent conservative estimates, since the perturbation force used to obtain these torques is unlikely to be observed during natural quiet standing.

Our theoretical analysis represents a crucial first step towards developing an FES system for arm-free standing. It implies that the energy spent due to the FES-elicited muscle contractions can be minimized with the determined optimal combination of active DOF, and that four variations of this combination exist from which an appropriate set can be chosen for a particular individual with paraplegia. However, many other challenges need yet to be addressed. These include the development of a balance sensor for sensory feedback; the compensation for FES induced muscle fatigue; and the identification of an appropriate closed-loop control strategy to regulate FES induced muscle contractions. Our team and many others are currently attempting to address these and other issues that stand in the way of the development and implementation of a system for FES-assisted standing.

In conclusion, FES-assisted, arm-free standing is theoretically feasible with respect to multi-body stability and physiological joint torque limitations. This is true even when only six out of twelve DOF in the lower limbs are actuated. Our findings are especially relevant for individuals with paraplegia who are potential users of FES-assisted standing technology, since the muscles actuating specific DOF are often denervated or difficult to access. Also, it is preferred to develop an FES system with less stimulation electrodes (i.e., an FES system for 6 DOF rather than for 12 DOF) in order to reduce system complexity and cost, but increase its reliability.

ACKNOWLEDGMENTS

This work was supported in part by the Canadian and Foreign Scholarships, the Canadian Fund for Innovation, the Canadian Institutes of Health Research, the Ontario Innovation Trust, the Ontario Ministry of Health and Long-Term Care, Toronto Rehab, and the Faculty of Medicine Dean's Fund, University of Toronto.

REFERENCES

[1] Veltink, P. H., and Donaldson, N., 1998, "A Perspective on the Control of FES-Supported Standing," IEEE Trans. Rehab. Eng., 6(2), pp. 109-112.

[2] Jaeger, R. J., 1986, "Design and Simulation of Closed-Loop Electrical Stimulation Orthoses for Restoration of Quiet Standing in Paraplegia," J. Biomech., 19(10), pp. 825-835.

[3] Khang, G., and Zajac, F. E., 1989, "Paraplegic Standing Controlled by Functional Neuromuscular Stimulation. I. Computer Model and Control-System Design," IEEE Trans. Biomed. Eng., 36(9), pp. 873-884.

[4] Matjacic, Z., and Bajd, T., 1998, "Arm-free Paraplegic Standing. I. Control Model Synthesis and Simulation," IEEE Trans. Rehab. Eng., 6(2), pp. 125-138.

[5] Abbas, J. J., and Chizeck, H. J., 1991, "Feedback Control of Coronal Plane Hip Angle in Paraplegic Subjects Using Functional Neuromuscular Stimulation," IEEE Trans. Biomed. Eng., 38(7), pp. 687-698.

[6] Jaime, R.-P., Matjačić, Z, and Hunt, K. J., 2002, "Paraplegic Standing Supported by FES-Controlled Ankle Stiffness," IEEE Trans. Neural Sys. Rehab. Eng., 10(4), pp. 239-248.

[7] Winter, D. A., 1990, Biomechanics and Motor Control of Human Movement, Wiley & Sons, New York, NY, Chap. 2-6.

[8] Yamaguchi, G. T., and Zajac, F. E., 1990, "Restoring Unassisted Natural Gait to Paraplegics via Functional Neuromuscular Stimulation: A Computer Simulation Study," IEEE Trans. Biomed. Eng., 37(9), pp. 886-902.

[9] Zajac, F. E., 1993, "Muscle Coordination of Movement: A Perspective," J. Biomech., 26(Suppl 1), pp. 109-124.

[10] Anderson, F. C., and Pandy, M. G., 2001, "Dynamic Optimization of Human Walking," J. Biomech. Eng., 123(5), pp. 381-390.

[11] Chao, E. Y., and Rim, K., 1973, "Application of Optimization Principles in Determining the Applied Moments in Human Leg Joint during Gait," J. Biomech., 6(5), pp. 497-510.

[12] Runge, C. F., Zajac, F. E., Allum, J. H. J., Risher, D., Bryson, A. E., and Honegger, F., 1995, "Estimating Net Joint Torques from Kinesiological Data using Optimal Linear System Theory," IEEE Trans. Biomed. Eng., 42(12), pp. 1158-1164.

[13] Bresler, B., and Frankel, J. P., 1950, "The Force and Moments in the Leg during Level Walking," Transactions on the ASME, 72, pp. 27-36.

[14] Cahouet, V., Luc, M., and David, A., 2002, "Static Optimal Estimation of Joint Accelerations for Inverse Dynamics Problem Solution," J. Biomech., 35(11), 1507-1513.

[15] Kuo, A. D., 1998, "A Least-Squares Estimation Approach to Improving the Precision of Inverse Dynamics Computations," J. Biomed. Eng., 120(1), pp. 148-159.

[16] Kim, J. Y., 2005, "3D Dynamic Modeling, Control Synthesis, and Controllability Analysis for FES-Assisted Paraplegic Standing," M.A.Sc. thesis, University of Toronto, Canada.

[17] Kim, J. Y., Popovic, M. R., and Mills, J. K., 2006, "Dynamic Modeling and Torque Estimation of FES-Assisted Arm-Free Standing for Paraplegics," IEEE Trans. Neural Sys. Rehab. Eng., 14(1), pp. 46-54.

[18] Levin, O., Mizrahi, J., and Shoham, M., 1998, "Standing Sway: Iterative Estimation of the Kinematics and Dynamics of the Lower Extremities from Force-Plate Measurements," Biol. Cybern., 78, pp. 319-327.

[19] Sias, F. R., and Zheng, Y. F., 1990, "How Many Degrees-of-Freedom Does a Biped Need?," Proc. IEEE Int. Workshop on Int. Robotics and Systems, 1, pp. 297-302.

[20] Denavit, J., and Hartenberg, R. S., 1955, "A Kinematic Notation for Lower-Pair Mechanisms based on Matrices," J. Appl. Mech., 77, pp. 215-221.

[21] Nakamura, Y., and Ghodoussi, M., 1989, "Dynamics Computation of Closed-Link Robot Mechanisms with Nonredundant and Redundant Actuators," IEEE Trans. Robotics and Automation, 5(3), pp. 294-302.

[22] Gollee, H., Hunt, K. J., and Wood, D. E., 2004, "New Results in Feedback Control of Unsupported Standing in Paraplegia," IEEE Trans. Neural Sys. Rehab. Eng., 12(1), pp. 73-80.

[23] Risher, D., Schutte, L. M., and Runge, C. F, 1997, "The Use of Inverse Dynamics Solutions in Direct Dynamics Simulations," J. Biomech. Eng., 119(4), pp. 417-422.

[24] Slotine, J. J., and Li, W., 1991, Applied Nonlinear Control, Prentice Hall, Englewood Cliffs, NJ, Chap. 9.

[25] Giakas, G., and Baltzopoulos, V., 1997, "A Comparison of Automatic Filtering Techniques applied to Biomechanical Walking Data," J. Biomech., 30(8), pp. 847-850.

[26] Pezzack, J. C., Norman, R. W., and Winter, D. A., 1977, "An Assessment of Derivative Determining Techniques used for Motion Analysis," J. Biomech., 10(5-6), pp. 377-382.

[27] Dumont, C. E., Popovic, M. R., Keller T., and Sheikh, R., 2006, "Dynamic Force-Sharing in Multi-Digit Task," Clin. Biomech., 21(2), pp. 138-146.

[28] Vette, A. H., Masani, K., and Popovic, M. R., 2007, "Implementation of a Physiologically Identified PD Feedback Controller for Regulating the Active Ankle Torque during Quiet Stance," accepted to IEEE Trans. Neural Sys. Rehab. Eng.

[29] Popovic, M. R., and Keller, T., 2005, "Modular Transcutaneous Functional Electrical Stimulation System," Med. Eng. Phys., 27(1), pp. 81-92.

[30] Marsolais, E. B., and Kobetic, R., 1988, "Development of a Practical Stimulation System for Restoring Gait in the Paralyzed Patient," Clin. Orthop. Rel. Res., 233, pp. 64-74.